Measurement of the Neutron-Proton Cross Section at 1.0 and 2.5 Mev*

R. E. FIELDS,† R. L. BECKER,‡ AND R. K. ADAIR§

University of Wisconsin, Madison, Wisconsin

(Received January 6, 1954)

The total cross section of hydrogen for 1.0- and 2.5-Mev neutrons has been determined by measuring the neutron transmission of samples of 2–2–4 trimethylpentane and graphite. Electrostatically analyzed protons from an electrostatic generator were used to bombard thin targets of tritium absorbed in zirconium to produce 2.5-Mev neutrons, and thin targets of Li_2O to produce 1.0-Mev neutrons. A gas-filled recoil counter served as neutron detector. For both cross-section determinations the geometry of the measurement was such that neutrons scattered from the samples at angles greater than 4.2° in the laboratory system were not detected. A pulse-height discriminator, biased to reject pulses from low-energy neutrons, reduced the background from room-scattered neutrons to less than one percent and eliminated effects of low-energy neutron groups from the $Li^7(p,n)$ reaction and the $O^{18}(p,n)$ reaction. Neutron energy spreads, primarily caused by the finite target thicknesses, were determined by measuring the widths of narrow neutron-scattering resonances in sulfur and carbon. The results of the cross-section measurements are: $\sigma = 2.525 \pm 0.009 \times 10^{-24}$ cm² at a neutron energy of 2.540 Mev, and $\sigma = 4.228 \pm 0.018 \times 10^{-24}$ cm² at a neutron energy of 1.005 Mev. These values, together with the values of a_t, a_s, and ρ_t given by Burgy, Ringo, and Hughes yield values of the singlet effective range in the shape independent approximation of $2.48 \pm 0.20 \times 10^{-13}$ cm from the 2.5-Mev measurement, and $2.56 \pm 0.25 \times 10^{-13}$ cm from the 1.0-Mev observations. These effective ranges are consistent with the proton-proton scattering data and the hypothesis of the charge independence of nuclear forces.

I. INTRODUCTION

THERE is limited evidence establishing the charge independence of nuclear forces. While the similarity of energy levels of mirror nuclei[1] strongly suggests the equivalence of neutron-neutron and proton-proton forces, there is not yet as much information on the equality of neutron-proton forces and the forces between like nucleons. Recent experiments by Bockelman et al.[2] have served to determine the states of isotopic spin one in N^{14} and in B^{10} which corresponds to the isotopic spin-one ground states of O^{14} and C^{14}, and to Be^{10} and C^{10}, respectively. If nuclear forces are charge independent these states will form charge triplets, split in energy only by Coulomb forces. Since the energy splitting of these states can apparently be accounted for by Coulomb forces, it seems improbable that nuclear forces are strongly charge dependent. An analysis of the effect of charge independence of nuclear forces on the electromagnetic transitions in light nuclei indicates also that charge-dependent forces are not important.[3,4] While the high-energy n-p and p-p scattering suggests a charge-dependent interaction,[5] the cross sections are not in contradiction with any rules based solely on charge independence.[6]

Information derived from high-energy scattering and from states of light nuclei concern the nucleon-nucleon interaction in states of various relative angular momenta. While this is advantageous inasmuch as velocity-dependent forces are effective only in states of angular momentum greater than zero, the complexity of the interaction makes a detailed analysis of the data difficult. At low energies the nucleon-nucleon interaction takes place almost entirely in the S state. Recent theoretical investigations using the effective range theory of Schwinger[7–9] have emphasized the usefulness of low-energy measurements on the n-p and p-p system in the determination of the possible charge dependence of the nucleon-nucleon potential. The effective-range theory shows that, up to energies of a few Mev, the nucleon-nucleon interaction for each spin state can be expressed in terms of two parameters, the scattering length a, and the effective range ρ. Charge independence then implies that the singlet n-p scattering length and effective range, a_s and ρ_s, should be equal to the p-p scattering length and effective range. Schwinger[10] has shown that the difference observed between the n-p scattering length and the p-p scattering length is to be expected because of the different magnetic moments of the neutron and proton. Since the singlet state of the nucleon-nucleon system is almost at resonance near zero energy, the scattering length is very sensitive to variations of the potential and the approximate equality of the scattering lengths suggests

[1] F. Ajzenberg and T. Lauritsen, Revs. Modern Phys. 24, 321 (1952).
[2] Bockelman, Browne, Buechner, and Sperduto, Phys. Rev. 92, 665 (1953).
[3] D. H. Wilkinson, Nature 172, 576 (1953).
[4] L. A. Radicati, Phys. Rev. 87, 521 (1952).
[5] R. S. Christian and H. P. Noyes, Phys. Rev. 79, 85 (1950).
[6] D. Feldman, Phys. Rev. 89, 1159 (1953).
[7] H. A. Bethe, Phys. Rev. 76, 38 (1949).
[8] J. M. Blatt and J. D. Jackson, Phys. Rev. 76, 18 (1949).
[9] E. E. Salpeter, Phys. Rev. 82, 60 (1951).
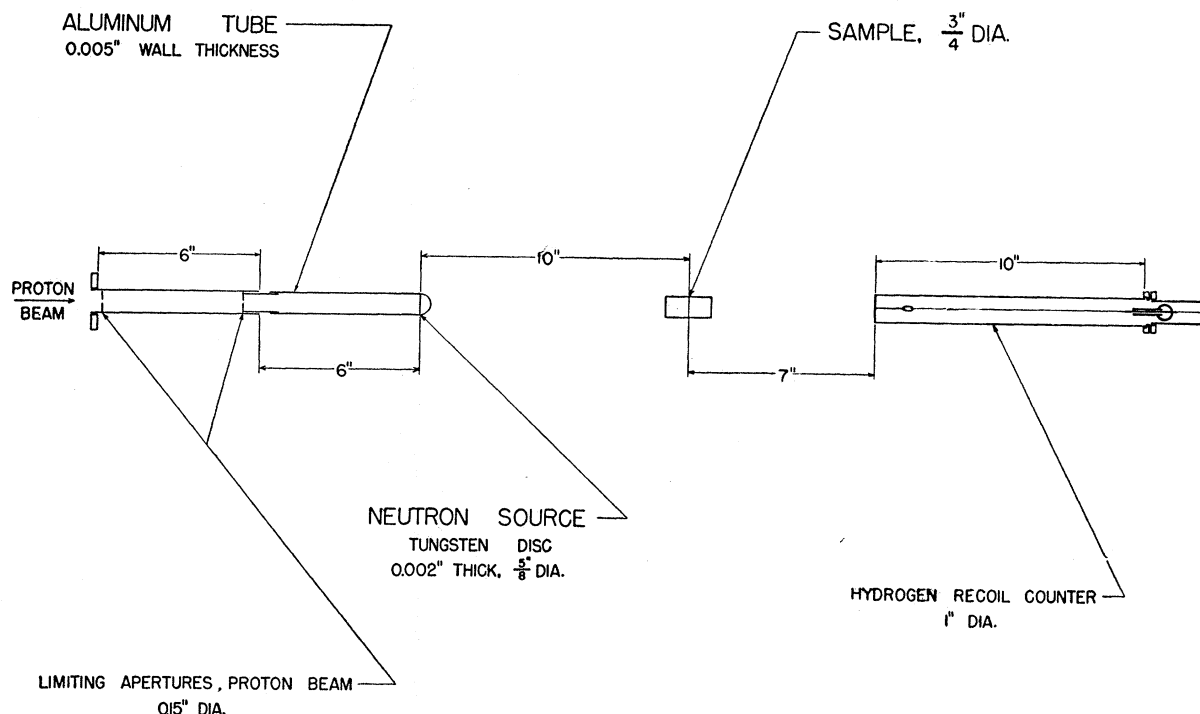[10] J. Schwinger, Phys. Rev. 78, 135 (1950).

FIG. 1. Schematic diagram of experimental arrangement.

strongly that the n-n and p-p forces are similar. It is, however, possible for two significantly different potentials to give the same scattering length and it is desirable to investigate whether the p-p and n-p effective ranges are the same.

The neutron-proton scattering cross section at low energies is made up of the sum of the triplet and singlet cross sections. The triplet contribution[11] can be calculated from accurately known values of a_t and ρ_t and subtracted from the measured total cross section to determine the singlet scattering which, at low energies, is a function of a_s and ρ_s only. Since a_s is known, ρ_s can then be determined. Salpeter has shown that previous low-energy measurements by Lampi et al.[12] indicate a singlet effective range of $2.6\pm0.5\times10^{-13}$ cm in the shape-independent approximation.

Recent accurate n-p cross-section measurements have been made at 5 Mev,[13] at 14 Mev,[14,15] and at 20 Mev.[16] At these energies the cross section depends sensibly on the shape of the potential, therefore the singlet range depends upon the assumptions made concerning the singlet and the triplet well shapes. Conversely, these experiments might be expected to provide information on the shape of the well if the

effective range is determined from experiments at lower energies. However, since $(v/c)^2$ is of the order of 3 or 4 percent at neutron energies of 15 or 20 Mev the uncertainties involved in the use of classical dynamics in the interpretation of these measurements may invalidate any very detailed conclusions.

The present experiments were performed to determine the shape-independent n-p effective range in an attempt to obtain further information on the charge dependence of nuclear forces. It was decided to perform cross-section measurements at 1.0 and 2.5 Mev. The difference in energy is sufficiently great that somewhat different techniques of measurement are necessary and the range derived from each measurement will be to some extent independent. This allows a check on the general reliability of the range determination. The effect of shape factors on the cross section at 1.0 Mev should be small, and at 2.5 Mev the shape correction will still be less than the experimental uncertainties.

II. APPARATUS

The measurement of the hydrogen cross section was made, in the case of both the 1.0-Mev and the 2.5-Mev measurements, by determining the relative neutron transmission of a hydrocarbon and of graphite. Figure 1 shows schematically the experimental arrangement. 1.0-Mev neutrons were produced by bombarding Li_2O targets of about 10-kev stopping power with electrostatically analyzed protons accelerated by an electrostatic generator. A target of tritium absorbed in a

[11] Burgy, Ringo, and Hughes, Phys. Rev. **84**, 1160 (1951).
[12] Lampi, Freier, and Williams, Phys. Rev. **80**, 853 (1950).
[13] Hafner, Hornyak, Falk, Snow, and Coor, Phys. Rev. **89**, 204 (1953).
[14] Poss, Salant, Snow, and Yuan, Phys. Rev. **87**, 11 (1952).
[15] Coon, Bondelid, and Phillips, quoted by Coon, Graves, and Barschall, Phys. Rev. **88**, 562 (1952).
[16] R. B. Day and R. L. Henkel, Phys. Rev. **92**, 358 (1953).

30-kev thick layer of zirconium was used to produce 2.5-Mev neutrons.

An important consideration in the design of the neutron source was to reduce to a minimum the number of low-energy neutrons produced by scattering in the source assembly. Most of these neutrons are produced by the primary Li(*p,n*) or T(*p,n*) reaction at angles other than 0° with respect to the incident proton beam, and are then scattered elastically in the forward direction by material in the immediate neighborhood of the source. Such neutrons are not counted as background because they are scattered from material near the primary source and cannot be distinguished from the primary beam. Since these scattered neutrons are produced initially at an angle with the proton beam, they have a lower energy than those emitted in the forward direction and therefore add a low energy component to the beam. In order to minimize the material near the source the targets were backed by a wolfram disk 0.002 in. thick. The disk was held in a vacuum housing of 0.005-in. aluminum.

The proton beam passed through two 2.4-mm collimation holes, spaced 15 cm apart, before striking the target. The target and vacuum housing, which are insulated from the collimation system by a length of Lucite, form a Faraday cage. The charge incident on the target was measured by a current integrator. Currents of about one microampere were used throughout both measurements. Since the energy developed in the targets could be dissipated only by radiation, the targets attained temperatures estimated to be about 400°C. It was, therefore, not possible to use lithium, which melts at about 184°C, as a target material. Targets of Li_2O prepared by allowing evaporated lithium to oxidize, proved stable under bombardment. The tritium-zirconium target, used for the 2.5-Mev determination, lost about 20 percent of its tritium in the 200 hours during which it was subjected to bombardment.

A high-pressure gas recoil counter was chosen as a detector, because it had been found in previous work that counters of this type have a high neutron sensitivity, and discriminate effectively against gamma rays. The counter consisted of a stainless-steel outer cylinder, one in. in diameter and 0.030 in. thick, with a 0.040-in. end cap. A 0.005-in. Kovar wire, entering the counter through a Kovar seal, was held at a positive potential. For the detection of 2.5-Mev neutrons, the counter was filled with 35 atmos of tank hydrogen, purified by passing it over palladized asbestos, through a liquid air trap, and over hot magnesium chips. The counter was operated as a pulse ionization chamber with the counter wire held at about 3500 volts. Pulses from the neutron recoils seemed to be somewhat reduced in size compared to those measured at lower gas pressures, possibly because of recombination.

The efficiency of the recoil counter as a function of

energy was measured by comparing the counting rates of the recoil counter with those of a long counter. The absolute sensitivity of the long counter was measured by determining the counting rate produced by neutrons from a calibrated radium-beryllium source. Since the electric field in the recoil counter varies considerably from the center wire to the counter wall, it seemed probable that recoils occurring in low field regions near the wall would be affected to a greater extent by recombination and produce a smaller voltage pulse than recoils occurring in high field regions near the wire. If such an effect is important, the efficiency of the counter will be smaller than the efficiency calculated from the known *n*-*p* cross section. The circles in Fig. 2 show the measured counter efficiency with the discriminator bias adjusted to the level used in the 2.5-Mev transmission measurements. The solid line represents the calculated efficiency neglecting end effects and the scattering of neutrons into and out of the active volume of the chamber by the end cap and counter walls. In view of the uncertainty of such effects the agreement of the measured and calculated values is satisfactory, indicating that there is no appreciable effect from recombination.

For the 1.0-Mev experiment it appeared desirable to use some gas multiplication to improve the signal-to-noise ratio. Satisfactory operation was obtained by filling the counter with 25 atmos of helium and 0.2 atmos of CO_2. A gas multiplication of about 5 was produced by operating at a voltage of about 3000. The efficiency of the counter is higher than that of a counter filled to the same pressure of hydrogen because of the large back-scattering cross section of helium for 1.0-Mev neutrons. The solid circles in Fig. 2 show the counter efficiency as a function of energy with the same discriminator bias as was used in the 1.0-Mev transmission measurements.
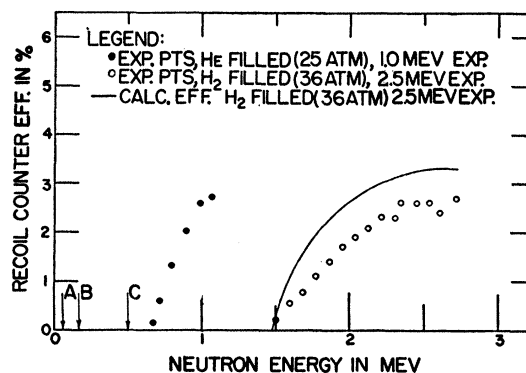

FIG. 2. Counter efficiencies. The solid points show the measured efficiency of the counter as used at 2.5 Mev and the solid curve is the theoretical efficiency. The efficiency of the counter as used at 1.0 Mev is shown by the circles. The three arrows *A*, *B*, and *C* refer to the measurements at 1.0 Mev. Arrows *A* and *B* represent the two groups of neutrons at 0° in the laboratory system from the $O^{18}(p,n)F^{18}$ reaction, while arrow *C* represents the neutrons from the reaction $Li^7(p,n)Be^{7*}$.

If the ionization produced in the counter sets up sufficient space charge to affect the gas multiplication, the counter efficiency might be expected to vary with counting rate. In an effort to determine whether such an effect was important, the neutron counting rate was measured when a 2-mg radium source was placed 10 cm from the counter. Through the radium γ rays produced a very high ionization density in the counter, the neutron counting rate was not affected.

During the 2.5-Mev measurement the neutron flux was monitored by a set of ten $B^{10}F_3$ proportional counters set in a block of paraffin. This monitor was placed 65 cm from the neutron source at an angle of 120° with the proton beam. It was observed in the course of the experiment that the monitor counting rate was accurately proportional to the proton current on the target. This showed that the effects of beam and target nonuniformity were very small, so that for the 1.0-Mev cross-section measurement the flux was monitored by measuring the charge incident on the target by means of a current integrator. Small fluctuations in the proportionality of neutron flux to incident proton current would be randomly distributed among carbon and hydrocarbon transmission measurements. Therefore, the only effect of such fluctuations on the data would be a greater dispersion of the cross-section values measured in individual runs than that indicated by statistical considerations.

III. ENERGY MEASUREMENT

Since the n-p cross section varies approximately as the square root of the neutron energy at the energies at which the cross-section measurements were made, it was necessary to determine the effective neutron energy accurately. For a uniform target the effective neutron energy and the spread in neutron energy can be calculated from the energy distribution of the incident protons, since the reaction energy is known. The effective neutron energy distribution will depend upon the characteristics of the electrostatic analyzer through which the protons pass, on the thickness of the target, and, for the higher-energy measurement, on the distribution of the tritium in the zirconium.

It had previously been noted at this laboratory[17] that in some tritium-zirconium targets the tritium was not distributed uniformly through the zirconium. In particular, there was sometimes little tritium in the top of the zirconium layer. To avoid errors which might arise from an incomplete knowledge of the target thickness and uniformity, it appeared desirable to make a more direct measurement of the effective neutron energy and the neutron-energy distribution. It is possible to determine the shape of the neutron-energy distribution by measuring the yield from a neutron-induced reaction at a very narrow resonance as a function of the incident-proton energy. By increasing

the proton energy in small steps, ΔE_p, the neutron-energy spectrum can be moved past the resonance in small steps, ΔE_n, where $\Delta E_n \approx \Delta E_p$ if E_p is far enough above threshold. The resonance, if it is narrow compared to the width of the neutron-energy distribution, may be regarded as a detector which picks out of the spectrum neutrons with a particular energy. Therefore a measurement of the yield as a function of E_p enables one to determine the neutron spectrum.

Bockelman et al.[18] have found a resonance, about 8 kev wide, for the scattering of 2.08-Mev neutrons by carbon which could be used to determine the mean energy and the energy spread of the neutrons from the tritium target. An accurate measurement was made of this resonance energy so the resonance could be used as a neutron-energy standard. A thin lithium target was evaporated in place and used to measure the transmission of carbon at this resonance. Resolution slits on the electrostatic analyzer were adjusted so that the proton energy half-width was about 2 kev.

Values of the transmission are shown by solid circles in Fig. 3. The abscissas of the figure represent potentiometer readings which are proportional to the voltage across the analyzer plates and hence to the proton energy. Crosses on Fig. 3 represent the counting rate as a function of proton energy at the Li(p,n) threshold using the H_2^+ beam from the generator. This threshold measurement establishes the absolute energy scale for the 2.5-Mev measurement. Excepting small corrections for relativistic effects and the mass of the electron in the H_2^+ ion, the energy scale represented by the abscissa of Fig. 3 for the threshold measurement is just one-half of that for the transmission measurement. A nonlinearity of the analyzer would not affect the energy measurement as the
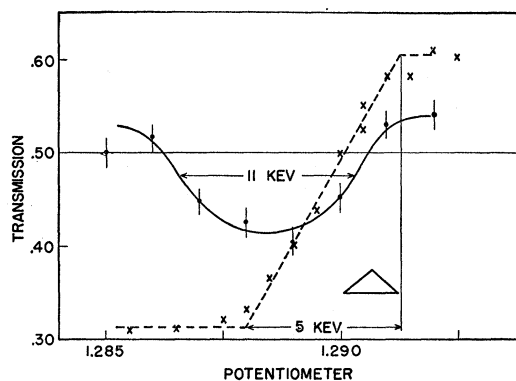

FIG. 3. Energy of carbon resonance. The broken line (crosses) represents the threshold rise curve of neutron counting rate, obtained by bombarding a thin lithium target with molecular hydrogen ions. The solid line (solid circles) shows the transmission of a carbon sample measured with neutrons obtained by bombarding the lithium target with protons. The abscissa represents a potentiometer reading which is proportional to the voltage across the plates of the electrostatic analyzer.

[17] Williamson, Browne, Craig, and Donahue, Phys. Rev. 84, 731 (1951).

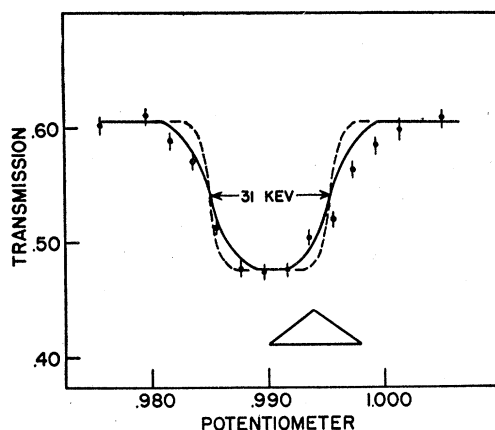[18] Bockelman, Miller, Adair, and Barschall, Phys. Rev. 84, 69 (1951).

FIG. 4. Carbon resonance observed with the tritium target. The experimental points represent the transmission of a carbon sample measured with neutrons obtained by bombarding the tritium target with protons. The solid curve shows the transmission calculated if the target were uniform and 31 kev thick, while the dotted curve shows the transmission shape expected if the resonance were very narrow, and hence is a measure of the neutron-energy spectrum.

analyzer voltage is almost exactly the same for the transmission measurement and for the threshold determination. However, a measurement of the Li(p,n) threshold using the proton beam was in agreement with previous measurements establishing the linearity of the analyzer system. Taking the Li(p,n) threshold as 1.8815±0.001 Mev,[19] the carbon-scattering resonance occurs at a neutron energy of 2.087±0.0035 Mev. The stated error arises from an uncertainty of 2 kev for the value of the center of the resonance, of 2 kev in the energy scale, and about one kev for the half-thickness of the lithium target. The target thickness was estimated as 5 kev for 2-Mev protons from the measured rise of counting rate at threshold.

Results of a transmission measurement at the same resonance using the tritium target are shown in Fig. 4. The solid circles represent the measurements. If the width of the resonance were negligible, the deviation of the points from the constant background would be nearly proportional to the actual neutron-energy distribution. Tritium evenly distributed in a zirconium layer 31 kev thick for protons of this energy would produce a transmission curve shown by the solid line. This curve, which includes the effects of the finite width of the resonance level, appears to be in fair agreement with the experimental points. The dashed curve shows the neutron-energy distribution from such tritium target.

From the kinematics of the T(p,n) reaction[20] it is possible to calculate the proton energy required to produce 2.087-Mev neutrons. This will be the energy of protons at the half-thickness of the zirconium-

tritium target. Comparison of this value with the incident proton energy determined from the voltage on the plates of the electrostatic analyzer indicated that there was no appreciable layer of either carbon or nontritiated zirconium at the surface of the target.

The neutron-proton cross section was measured at a neutron energy about 450 kev higher than the carbon-scattering resonance. From the T(p,n) kinematics the increase in proton energy required to reach this neutron energy was calculated. As the increase in proton energy was not large, the change in stopping power of the zirconium was small and the neutron-energy spectrum should be similar to the spectrum determined at 2.08 Mev shown by the dashed line in Fig. 4. Assignment of the effective neutron energy was made from the measured neutron energy at the carbon resonance and the knowledge of the increase in proton energy.

It was concluded that the mean energy of the neutrons used in the cross-section measurement was 2.540±0.006 Mev and the shape of the distribution was essentially that shown by the dashed line in Fig. 4 with a full width of about 30 kev. The error is primarily the result of uncertainties in determination of the center of the distribution, and the error assigned to the energy of the carbon resonance. Table I shows an estimate of all uncertainties affecting the assignment of the error in the energy determination.

At 1.0 Mev the Li(p,n) reaction appeared to be more suitable as a neutron source than the T(p,n) reaction as it was possible to prepare lithium targets which gave a greater neutron yield per kev stopping power, and the low-energy group of neutrons from this reaction could be effectively biased out. It is probable that in the preparation of the Li_2O targets which were used in these experiments some Li_2CO_3 and LiOH were formed. Originally the targets were light gray in color, but they turned white after a brief bombardment by the proton beam. It is believed that most of the water and carbon dioxide was driven off by the heat produced by the beam. The thickness of the Li_2O targets was measured by determining the rise of the yield at threshold and, more reliably, by measuring the experimental width of the 1.5-kev wide neutron-

[19] Jones, McEllistrem, Douglas, and Richards, Phys. Rev. **91**, 482 (1953).
[20] Taschek, Argo, Hemmendinger, and Jarvis, Phys. Rev. **76**, 325 (1949).

TABLE I. Uncertainty in energy measurement (in kev).

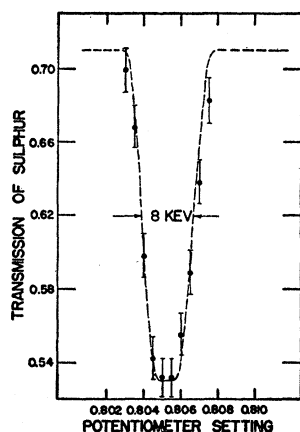|	2.1-Mev carbon resonance	1-Mev *n-p* measurement	2.5-Mev *n-p* measurement	1.3-Mev oxygen resonance
Energy of Li(p,n) threshold	2	1		1
Energy of 2.1-Mev carbon resonance			3.5	
Target thickness	1.5	1.5	3	1.5
Setting for Li(p,n) threshold	2	2		2
Setting for 2.1-Mev carbon resonance			3	
Total (rms)	3.5	3	5.5	3

FIG. 5. Lithium oxide target thickness. The curve represents the variation of the transmission of sulfur expected from a target 8 kev thick, the points represent the measured transmissions.

scattering resonance in sulfur at 587 kev.[21] The circles in Fig. 5 show the measured transmission at this resonance with one of the two targets used in the 1.0-Mev cross-section measurement, and the dashed curve shows the transmission expected from a target 8 kev thick with allowance for the spread in energy of the proton beam and the width of the resonance. The measured transmission appears to show an asymmetry indicating a possible nonuniformity of the target thickness. An examination of the Li_2O surface under a microscope supports the view that the surface is sufficiently roughened by the formation of crystalline grains to produce such an effect. This asymmetry is not sufficiently large to affect the measurement adversely.

The n-p cross-section measurement was made at 1.005±0.003 Mev. This energy was calculated from the kinematics of the $Li(p,n)$ reaction and the measured proton energy. Most of the error assigned to the energy is due to the uncertainties in the target thickness and in the stability of the voltage supply of the electrostatic analyzer. Estimates of the contributions of these errors are made in Table I. Electrostatic analyzer dynamics and reaction kinematics were calculated relativistically throughout. Storrs and Frisch[22] have measured the n-p cross section at a neutron energy of about 1.31 Mev. They used a scattering resonance in oxygen at this energy as a reference point and determined its energy to be 1.314 Mev. It appeared desirable to make an independent measurement of this energy to relate more clearly the present measurements to those of Storrs and Frisch, and to establish another point for comparison of neutron-energy measurements. The circles in Fig. 6 are the results of measurements of the transmission of a BeO sample at this resonance using as a neutron source the same Li_2O target that was used for most of the 1-Mev n-p cross-section experiment. The

[21] Peterson, Barschall, and Bockelman, Phys. Rev. **79**, 593 (1950); Kiehn, Goodman, and Hansen, Phys. Rev. **91**, 66 (1953). The results of Peterson *et al.* made at this laboratory, give a resonance energy of 587 kev, recalculated using relativistic dynamics. Kiehn *et al.* quote a value of 588 kev.

[22] C. L. Storrs and D. H. Frisch, Phys. Rev. **90**, 339 (1953) and private communication.

location of the same resonance was also determined by use of a fresh 3-kev metallic lithium target. The two measurements, which differed by less than a kilovolt, yielded the value 1.315±0.003 Mev for the position of the oxygen resonance. Table I shows an estimate of the uncertainties which make up the assigned error.

In considering the effective energy of the sources used in this experiment it is necessary to include the presence of low energy neutrons which originate very near the source. There will be two sources of such neutrons. They may be produced in the primary reaction at an angle with the incident proton beam and subsequently scattered in the forward direction into the detector, or in reactions other than the primary reaction.

Two groups of low-energy neutrons produced by extraneous reactions result from the bombardment of Li_2O by protons. Arrows on Fig. 2 show the energy of neutrons produced by the $Li^7(p,n)Be^{7*}$ reaction and the $O^{18}(p,n)F^{18}$ reaction. Pulses from neutrons of both these reactions will be rejected by the pulse-height discriminator. Though no (p,n) reaction of a stable nucleus can produce neutrons of appreciably higher energy than the $T(p,n)$ reaction, it appears possible that low-energy neutrons might be produced in small numbers by the bombardment of zirconium or wolfram by protons. A measurement of the intensity of such neutrons was made by bombarding a target of zirconium of about 100-kev stopping power evaporated onto a wolfram backing with 3.5-Mev protons and observing the neutron flux with the recoil counter under conditions similar to those used to detect the $T(p,n)$ neutrons. The counting rate produced in this way was less than 0.1 percent of that caused by the $T(p,n)$ neutrons used in the cross-section measurement.

Neutrons produced by the $T(p,n)$ reaction at angles greater than about 70° with respect to the proton beam, or by the $Li(p,n)$ reaction at angles greater than about 80°, have too small an energy to be registered by the counter. However, those emitted at smaller angles but with energies large enough to be counted, can be scattered into the forward direction by the wolfram target backing and by the aluminum vacuum housing.
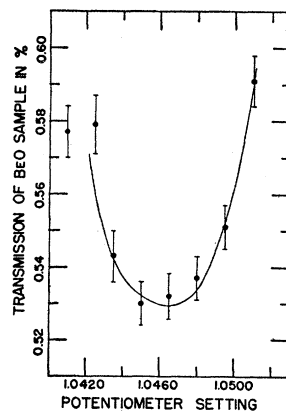

FIG. 6. Energy measurement of 1.31-Mev oxygen resonance. The circles show the transmission of a BeO sample measured with an 8-kev Li_2O target.

An estimate of the fraction of the measured flux resulting from this effect was made assuming that the differential cross sections for scattering by wolfram and by aluminum are equal to the total cross sections divided by 4π and that the neutrons are emitted isotropically by the source. The scattered flux was integrated over the portions of the target backing and aluminum vacuum housing from which neutrons could be scattered into the detector with sufficient energy to be recorded. This calculation indicated a contribution of about 0.2 percent of lower energy neutrons for the measurement at 1.0 Mev and considerably less for the measurement at 2.5 Mev. When the counter sensitivity and the small variation of the hydrogen cross section are taken into account, it appears that the effect of these neutrons on the measured cross section can be safely neglected.

IV. CROSS-SECTION MEASUREMENT

The cross section was measured by determining the ratio of the transmission of a thin-walled cylindrical aluminum container filled with 2–2–4 trimethylpentane, $(CH_3)_3CCH_2CH(CH_3)_2$, to the transmission of a similar container holding a graphite cylinder which had the same number of carbon nuclei per square cm as the hydrocarbon samples. Under conditions of good geometry the $n-p$ cross section for monoenergetic neutrons is then equal to $-(1/N)\ln T$, where N is the number of hydrogen atoms per cm^2 in the hydrocarbon scatterer and T represents the ratio of the transmission of the hydrocarbon scatterer to that of the carbon scatterer. It is unnecessary to measure separately either the carbon cross section or the attenuation of the beam by the containers.

The trimethylpentane was obtained from Eastman Kodak; the "spectro" grade, which was used, is stated by the supplier to contain less than 0.1 percent impurities. Using a specific gravity bottle, the density of the liquid as a function of temperature was found to be $0.6921[1+0.0013(20°-t)]\pm0.0003$ g/ml, in agreement with the handbook value. Since the most probable impurities are hydrocarbons with carbon-hydrogen ratios similar to trimethylpentane, the impurities will probably introduce a negligible error. For similar reasons the presence of dissolved water cannot affect the validity of the measurement. It was, however, necessary to monitor the temperature of the liquid carefully because of the large thermal expansion coefficient. The temperature of a brass block on which the sample rested during measurements on the carbon sample and of the background was measured to within 0.2°.

The aluminum containers were cylinders of 0.75-in. inside diameter with walls 0.005 in. thick. For the 2.5-Mev measurement the scatterer was about 4.4 cm long and had end caps of aluminum 0.005 in. thick which were waxed into place. The scatterer used for the 1.0-Mev measurement was about 3 cm long and had end caps of 0.005-in. tantalum. The length of the scatterers was measured with a caliper the opening of which was determined using a traveling microscope. The engine screw of the microscope had been calibrated with standard meter bar BS No. 210. Individual determinations of the length of the scatterer were reproducible to within 0.0003 cm. Since the end caps were not perfectly flat or parallel, measurements were made at many points on the end surfaces. The mean deviation of the thickness along the axis was about 0.0020 cm. An average length was computed from these measurements. When the transmission measurements at 2.5 Mev were in progress it was noted that the cylinder dimensions were not completely stable under the necessary handling involved in changing samples. The average length of the sample varied by as much as one part in a thousand from day to day, though the mean deviation was about one-half of this. The greater strength of the tantalum end caps used on the scatterer for the 1.0-Mev measurement resulted in much greater dimensional stability of that sample. Carbon scatterers were machined from spectroscopically pure graphite rods obtained from the National Carbon Company. Density of the graphite was measured to be 1.48 g/cm³ for several samples, indicating no appreciable variation in density through the cylinders. Since the scatterers did not change weight appreciably when heated, it was concluded that large amounts of absorbed gases were not present.

The scatterers rested in position on a light wire cradle mounted on a thin vertical rod supported by a base on the floor. Alignment was checked periodically by placing on the cradle a Lucite tube, of the same outside diameter as the scatterers and a length equal to the distance from the source to the face of the counter. Deviations of the centers of the source, sample, and counter, of 1 mm from a straight line were easily detected and corrected. Since the number of atoms per cm^2 in the scatterer varies inversely as the cosine of the angle between the axis of the scatterer and the beam direction, it is necessary to align the scatterer accurately. With the aid of the Lucite tube deviations of one degree could be observed. Alignment checks were made continually throughout the measurements.

Background counts, resulting mainly from room-scattered neutrons, were determined by measuring the counting rates with the primary beam of neutrons blocked out by scatterers of paraffin or Lucite. A Lucite cylinder, 35 cm long, having a calculated transmission of 0.001 was used to shield the direct beam to determine the background for the 2.5-Mev measurement. The magnitude of this background was about 0.6 percent of the counting rate from the unshielded direct beam. A paraffin cone 30 cm long with a negligible calculated transmission was used in the same way to show that the background at 1.0 Mev was about 0.8 percent.

Cross sections calculated on the assumption that

attenuation by the scatterer is an exponential function of the length of the scatterer are subject to errors caused by the hardening effect and by neutrons scattered into the detector by the sample. The hardening effect is the result of variation of the cross section over the finite neutron-energy spread. Neutrons on the low-energy side of the spectrum are scattered with slightly higher probability than those on the high side. Therefore the mean energy increases as the beam passes through the scattering sample. The result is a rate of decrease of intensity slightly less rapid than exponential.

Calculation of the cross section from a measured average transmission for finite neutron-energy spread, assuming exponential attenuation, therefore, yields a value less than or equal to the true cross section averaged over the energy spread. The equality holds in the limit of vanishing attenuation or if the cross section is independent of energy. In the present experiments the hydrogen cross section changes about $\frac{1}{2}$ percent over the energy spectrum. The resulting error is only about 0.02 percent.

The error caused by neutrons scattered into the detector by single collisions in the sample is given by

$$\frac{\delta\sigma}{\sigma} = \frac{g}{4} \cdot \left[\frac{r(D_1+D_2)}{D_1 D_2}\right]^2, \tag{1}$$

where r is the radius of the scatterer, T is its transmission, D_1 is the distance from the source to the scatterer, and D_2 is the distance from the scatterer to the detector.

$$g = \left(\frac{d\sigma}{d\omega}\right)_{0°} \Big/ \frac{\sigma_t}{4\pi},$$

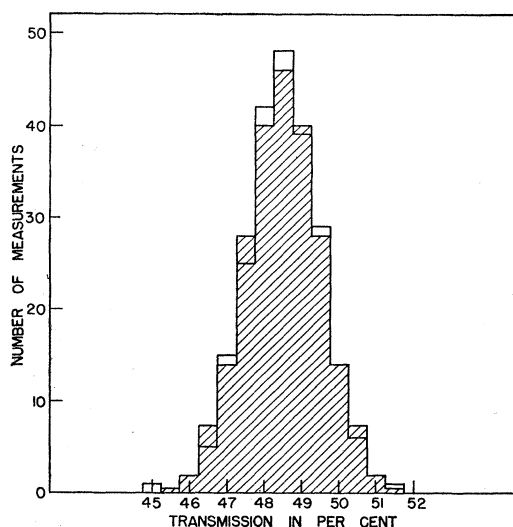i.e., g is the differential cross section at 0° divided by

FIG. 7. Histogram of 224 transmission measurements at 2.5 Mev. The frequency is plotted against the transmission. The cross-hatched area represents the "probable" histogram calculated from the number of counts recorded.
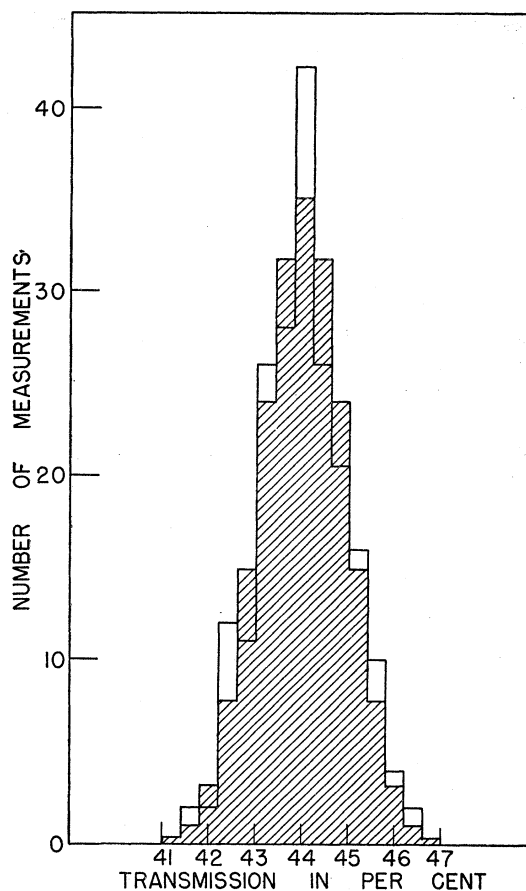

FIG. 8. Histogram of 200 transmission measurements at 1.0 Mev. The frequency is plotted against the transmission. The cross-hatched area represents the "probable" histogram calculated from the number of counts recorded.

the average differential cross section averaged over all directions; it is equal to 4 for hydrogen. Values of g for carbon are somewhat uncertain. At 2.5 Mev, $g=4$ was selected on the basis of published measurements of the angular distribution of neutrons scattered from carbon,[23] while at 1.0 Mev, $g=2.5$ was used. In-scattering effects from carbon cancel out to some extent so that the uncertainty in angular distribution has only a small effect on the in-scattering correction applied to the relative transmission.

The calculated value of $\delta\sigma/\sigma$ is 0.008 for the 2.5-Mev measurement and 0.007 for the 1.0-Mev measurement.

Neutrons reaching the detector after more than one collision in the scatterer constitute a fraction less than $(1 - T - T\ln T)g d\omega$ of the direct beam, where $d\omega$ is given by $\frac{1}{4}[r(D_1+D_2)/D_1 D_2]^2$. In the present experiments this amounts to about two-thirds of the fraction singly in-scattered. However, if the effect of energy degradation on the detection efficiency for the multiply in-scattered neutrons is taken into account it appears that

---

[23] Baldinger, Huber, Ricamo, and Zunti, Helv. Phys. Acta 23, 503 (1950).

the net correction for multiple in-scattering is not more than one-tenth of the correction for single in-scattering.

Transmissions were determined at each energy by making over 200 individual measurements, each of which determined the cross section with a statistical standard error of 2.7 percent. Figures 7 and 8 show the distribution of these measured transmissions, together with normal distributions calculated from the number of counts recorded in each measurement. The standard errors in the averages of the experimental measurements are 0.14 percent at 2.5 Mev and 0.17 percent at 1.0 Mev. The standard errors predicted from the number of counts were in each case almost exactly the same. This good agreement between the errors calculated from the individual measurements and from the number of counts indicates that any random variation of experimental conditions, such as fluctuations in the electronic circuits, does not seriously affect the accuracy of the measurements.

Counting rates were less than 30 counts per second for the 2.5-Mev experiment and 20 counts per second at 1.0-Mev. The amplifier had a rise time of 0.5 μsec, and clipping times of 2 μsec and 4 μsec were used in the 2.5- and 1.0 Mev experiments, respectively. Measurements with a double pulse generator gave a resolution of 5 μsec for the discriminator. The portion of time during which the counter system is dead will be equal to $2Nt$, where N is the number of counts/second and t is the recovery time of the system. The time t will be about equal to the time a pulse stays above the discriminator level plus the recovery time of the discriminator. This recovery time will depend upon the height and shape of the pulse. For the conditions of this experiment the average value of t will be a little less than the sum of the discriminator time constants and the amplifier clipping time constant. Pulses smaller than the setting of the discriminator will be occasionally superposed and register as a count. The fraction of pulses produced by this "pile up" will be equal to $2N't'$, where the average value of t' depends on the shape of the pulses and upon the pulse spectrum, and N' represents the number of pulses per second which are too small to trigger the discriminator. N' is not greatly different from N and the effective value of t' is estimated to be about 2 μsec. The two corrections, for dead time and for pile up, are in opposite directions

TABLE II. Sources of error in cross-section measurement (in parts per thousand).

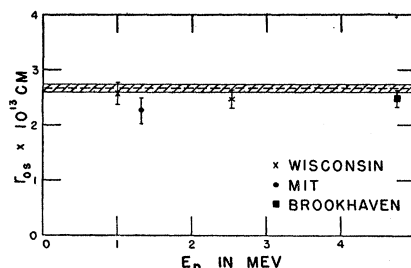|	2.5-Mev measurement	1.0-Mev measurement
Statistical standard error	1.9	2.3
Energy	1.9	1.5
Background	1.2	1.6
In-scattering	1.3	1.6
Nuclei/cm²	1.5	1.6
Total (rms)	3.5	4.0

FIG. 9. Singlet effective range vs energy. The points at 1.0 and 2.5 Mev represent effective ranges calculated from the present measurements. The 1.3-Mev and 5-Mev points show ranges calculated from the work of the MIT group and the Brookhaven group, respectively. The errors shown reflect only the uncertainties in the $n-p$ cross-section measurements. The dashed line shows the proton-proton effective range.

and have an effect of only about 0.03 percent on the cross section.

V. RESULTS AND DISCUSSION

Evaluation of the two cross-section measurements results in a neutron-proton total cross section of 2.525 ± 0.009 barns at a neutron energy of 2.540 Mev, and a value of 4.228 ± 0.018 barns at 1.005 Mev, where the quoted errors represent standard deviations. Table II lists the important sources of error and estimates of their magnitudes in terms of parts per thousand of the cross section. The uncertainty in neutron energy is treated as an uncertainty in cross section at an exact neutron energy. The resultant total error was taken as the root mean square of the individual errors.

From these values of the cross sections a value of the neutron-proton singlet effective range can be derived and compared with values calculated from neutron-proton cross sections obtained by other workers, and with the proton-proton effective range. Singlet effective ranges were calculated in the shape-independent approximation using the relationship

$$\sigma = \frac{3\pi}{k^2+(1/a_t-\frac{1}{2}\rho_t k^2)^2} + \frac{\pi}{k^2+(1/a_s-\frac{1}{2}\rho_s k^2)^2}, \quad (2)$$

where k is the neutron wave number, a_t and a_s are the triplet and singlet scattering lengths, and ρ_t and ρ_s are the corresponding effective ranges. Values of a_s, a_t, and ρ_t were taken from the paper of Burgy et al.[11] At the energies used in this experiment the relativistic corrections to k are small. k^2 was, therefore, calculated from $k^2=2\mu E/\hbar^2$ where E represents the energy of the system in center-of-mass coordinates and μ the reduced mass. The singlet effective range calculated from the 2.5-Mev cross-section measurements is $2.48\pm0.20 \times 10^{-13}$ cm; while the 1.0-Mev measurement leads to a value of $2.56\pm0.25\times10^{-13}$ cm. The errors assigned to the two determinations include uncertainties in the parameters a_s, a_t, and ρ_t as well as the measured cross sections and are, therefore, not independent. Assuming

the validity of the shape-independent approximation the close agreement of the two effective range values is evidence for the reliability of the cross-section measurements.

Figure 9 shows the values of singlet effective ranges, calculated on the shape-independent approximation from recent cross-section measurements, plotted as a function of the neutron energy at which the measurements were made. The errors shown represent only the independent errors in the cross section measurements and do not include the uncertainties in the parameters

a_s, a_t, and ρ_t. Figure 9 shows excellent agreement between the various measurements.

The dashed line in Fig. 9 represents the value of the proton-proton effective range[24,25] which is taken as $2.65 \pm 0.07 \cdot 10^{-13}$ cm. Though the calculated neutron-proton singlet effective ranges appear to be a little smaller than the proton-proton ranges, the agreement is within the errors of the experiments and constitutes evidence for the charge independence of nuclear forces.

[24] J. D. Jackson and J. M. Blatt, Revs. Modern Phys. 22, 77 (1950).
[25] H. H. Hall and J. L. Powell, Phys. Rev. 90, 912 (1953).

Atomic Masses in the Intermediate Region*

T. L. Collins, Walter H. Johnson, Jr., and Alfred O. Nier
Department of Physics, University of Minneapolis, Minnesota†
(Received January 7, 1954)

The double-focusing mass spectrometer previously described has been used to measure 28 atomic masses in the region between gallium and niobium. The new information combined with previous determinations permits one to draw a rather complete packing fraction curve for the region from sulfur through xenon. Analysis shows that masses for stable and unstable isotopes of an element can be fitted by parabolas, one for odd A and one for even A. The two parabolas have the same shape (except just above a proton shell) but are displaced in A as well as mass. The displacements are such that, for an isobar, the minimum mass does not occur at the same Z for the four nuclear families (even even, etc.), in contradiction to usual assumptions.

THIS paper presents the results of a portion of an extensive program of mass measurement undertaken with the double-focusing mass spectrometer[1] developed at the University of Minnesota. Previous communications have covered the regions sulfur to zinc[2,3] and palladium to xenon,[4] as well as detailed studies of the triple isobars at mass 40 and 50.[5,6] We now report 28 mass doublets covering isotopes from gallium, $Z=31$, to niobium (columbium), $Z=41$. The combined data is now sufficient to reveal patterns and shell effects which are discussed under the heading of Mass Systematics.

DOUBLET MEASUREMENTS

The method of measurement has not been changed. We measure the atomic mass difference of two ions of the same mass number (a mass doublet). One ion has a known mass—it is usually a hydrocarbon fragment.

The ion current is detected electronically, and because of the nature of the feedback arrangement of the control circuits, the measurement of the mass difference reduces to a measurement of a resistance ratio.[2,7] A "run" consists of at least 10 consecutive tracings of the mass spectrum with alternate forward and backward sweep. Runs were taken on different days over a period of months. During these measurements, the width at half height of a mass "peak" corresponded to 1/10 000 of the ion mass. At these masses this resolution is insufficient to separate the C^{13} satellite (one less hydrogen) from the hydrocarbon peak. A correction is possible by measuring the relative intensity of the hydrocarbon ion at the next lower mass number, and where necessary this correction has been applied.

Table I lists the results of the doublet measurements. The errors are probable errors, and are purely statistical. The day-to-day variation usually exceeds that expected from the statistics within the runs. In this case a simple average is computed; otherwise a weighted average is used.

Several stable isotopes are missing. Selenium ions were reliably obtained only from H_2Se gas with the result that Se^{77} and Se^{78} were accompanied by incompletely resolved selenides of other isotopes. Krypton

[1] E. G. Johnson and A. O. Nier, Phys. Rev. 91, 10 (1953).
[2] Collins, Nier, and Johnson, Phys. Rev. 84, 717 (1951).
[3] Collins, Nier, and Johnson, Phys. Rev. 86, 408 (1952).
[4] R. E. Halsted, Phys. Rev. 88, 666 (1952).
[5] W. H. Johnson, Phys. Rev. 87, 166 (1952).
[6] W. H. Johnson, Phys. Rev. 88, 1213 (1952).
[7] A. O. Nier and T. R. Roberts, Phys. Rev. 81, 507 (1951).